Dynamic Strategy Selection for Physical Robotic Assistance in Partially Known Tasks

José Ramón Medina, Martin Lawitzky, Adam Molin and Sandra Hirche

***Abstract*— It is well-known that physical robotic assistance to humans is significantly enhanced by including human behavior anticipation into robot planning and control. The challenge arises when the human goal/plan is uncertain or unknown to the robot. In this paper we propose a novel control scheme which dynamically selects between a model-based and a model-free strategy depending on the level of disagreement between the human and the robot. The disagreement is measured in terms of the interaction force. A task specific model-based controller is selected when the human's motion intention coincides with the robot's goal. A model-free control scheme based on the human force as motion prediction source is selected in case of disagreement and when the human goal/plan is unknown. The benefits of this approach are demonstrated in a human user study on human-robot cooperative object transport through a 2D maze in virtual reality.**

I. Introduction

Physical robotic assistance to humans has a wide diversity of application scenarios such as mobility assistance or joint transportation. From human studies it is well-known that anticipation of the partner's action is key for successful joint action [1]. This holds also true for physical robotic assistance to humans as recent results show: a *proactive* anticipatory control is shown to outperform classical *reactive* approaches regarding human effort and subjective quality of assistance [2]. Such control schemes rely either on human motion prediction models or on pre-planned strategies based on a *previously known* common goal. However, the abilities of a robotic helper exhibiting anticipatory behavior should not be limited to assisting its partner in a set of tasks where human motion models, the environment and the desired goal are previously determined. The human's goal and the environment are not typically known in advance. They might be completely unknown or subject to dynamic changes producing additional uncertainties. In such cases, a flexible and helfpul artificial assistant should be able to infer the most suitable control strategy and even anticipate its partner's intentions during *unknown* situations.

As a proactive physical helper requires predictive capabilities, the field of anticipatory assistance covers a wide spectrum of *model-based* human behavior prediction methods ranging from simple human motion models to goal-oriented task-specific preplanned paths. In the simplest case, the well-known minimum-jerk principle for free-space motion of human arm movement [3] is used to extrapolate the human desired short-term motion trajectory and intermediate goal [4]. During cooperative manipulation tasks, a polynomial extrapolation becomes more suitable [5]. However, when a known common goal is available, planning-based methods estimate a desired path by minimizing the distance to the goal [6], [7]. Formulating the planning solution as a feedback law, feedback motion plans [8], [9] provide a more responsive anticipation during task execution as all possible paths are computed in advance. While planning-based approaches produce accurate goal-oriented behavior, they operate on kinematic level and neglect the task dynamics. As an alternative, learning-based approaches can be utilized to acquire implicit knowledge of the task dynamics [10], [11]. Acquiring human behavior models through teleoperation [12], [13] or in an incremental fashion during interaction [14], [15], the human partner is supported in an intuitive and human-adapted fashion by reproducing previously observed motions. Learning techniques provide a way to increase the robot's task-solving repertoire through experience but are only effective when previous task-specific experiences are available. All the above-mentioned model-based human motion prediction methods predict successfully their partner's behavior but require specific task information in advance. When human behavior diverges from any of the possible task specific plans known to the robot, a *model-free* anticipation strategy remains an open issue. Consequently, under human's plan or environmental uncertainty, a dynamic *selection* of the most appropriate strategy between all available model-based and model-free approaches arises as an additional problem.

The contribution of this paper is twofold. First, a model-free assistance scheme relying entirely on sensed forces is presented, becoming a suitable alternative when no specific task model coincides with the human intentions. Second, a method to select the most promising assistive strategy following a short-term retrospective evaluation methodology is presented. The proposed scheme estimates the applicability of both a model-based and the presented model-free control schemes based on recent prediction performance. Depending on the result, a strategy selection scheme decides to either retain the current assistance model or switch to a recently more successful strategy. A user study in a 2D virtual scene shows the applicability and the benefits the proposed approach in terms of human effort minimization.

The remainder of this paper is organized as follows: After we confine our problem in the next section, Section III describes our overall approach. Detailed explanations of our proposed assistive control schemes are given in Section IV. The experimental evaluation of our approach is described in

All authors are with the Institute for Information-Oriented Control, Department of Electrical Engineering and Information Technology, Technische Universität München, D-80290 Munich, Germany. {medina, ml, adam.molin, hirche}@tum.de

Section VI.

Notation: Bold symbols denote vectors. A multivariate normal distribution centered at $\boldsymbol{u}$ with covariance matrix Σ is denoted $\mathcal{N}(\boldsymbol{u}, \Sigma)$. The 2×2 and 4×4 identity matrices are denoted I_2 and I_4, respectively.

II. Problem Statement

The task considered in this work consists of the physically coupled movement of a human and a robot from an initial to a final configuration. However, instead of assuming cooperation towards a common goal known to both partners [16], [17], we additionally consider the possibility that the human diverges from the robot's assumed final configuration or path to the goal. No information on the desired trajectory of the human or the robot is provided to the partner other than through haptic interaction.

Depending on the application, the interaction between partners can be through an object, as in cooperative transportation, or in direct contact, as, e.g. in movement assistance tasks. For the sake of simplicity, here we consider the latter case, i.e. a common interaction point placed at the robot's end-effector. In order to provide the robot with a compliant *reactive behavior* allowing an intuitive reaction to the human force input, we implement an admittance-type control scheme. A *proactive behavior* aiming for human effort minimization is achieved adding an additional external force input to the admittance control. The system dynamics are therefore given by

$$M_r \ddot{\boldsymbol{x}} + D_r \dot{\boldsymbol{x}} = \boldsymbol{u_h} + \boldsymbol{u_r} \ , \tag{1}$$

with rendered inertia M_r and rendered viscous friction D_r, $\boldsymbol{u_h}$ the applied force by the human, $\boldsymbol{u_r}$ the assistive control input of the robot, and $\boldsymbol{\xi} = \begin{pmatrix} \boldsymbol{x} & \dot{\boldsymbol{x}} \end{pmatrix}^T$ the state of the system, where $\boldsymbol{x}$ denotes the position of the robot's end effector.

We further assume that the proactive robot contribution is calculated based on a task model λ in terms of the desired path, that, as stated in the problem conditions, can be close to the human intentions, incomplete, partially or completely wrong, i.e. we account for this possibility of divergence from the human side. The goal of this work is the synthesis of the anticipatory robot's proactive contribution $\boldsymbol{u_r}$ taking into account that the human may aim for a different goal or path than the active task model λ.

III. General Approach

From the problem setting, two different cases can be intuitively identified depending on the task model λ's similarity to the human intentions: a) when λ coincides with the human plan, or, in contrast b) the human's intended goal or path differs from λ. This binary case separation suggests the situation-dependent application of two different control schemes. On one side, an *model-based* control scheme relying on the task model's predictions performs satisfactorily when both partners have a similar plan (case a)). On the other, interpreting the human force as an indicator for the desired movement direction, a *model-free* control scheme based on the currently observed human control input is preferred when the human goal is unknown (case b)). Note, that an intermediate strategy between both cases is not considered as a useful solution since merging different goals can lead to undesired or even potentially unsafe configurations.

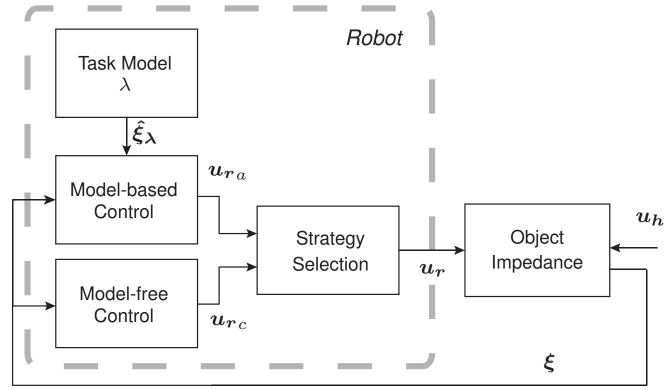

Fig. 1. General control scheme. The strategy selection switches between a model-based control scheme and a model-free control scheme depending on their performance in terms of human effort minimization.

We consequently propose a strategy selection approach that switches between the model-based and the model-free control based on their performance in terms of human effort minimization, as shown in Fig. 1. The resulting scheme supports the human partner in case of correct anticipation of the human's higher-level intention and also in unexpected situations.

IV. Assistive control schemes

In this section we propose two different strategies for motion generation in physical robotic assistance that implement feasible control schemes among which may be chosen.

An *ideal* robotic helper reduces the human partner's force contribution to 0 by perfectly anticipating the human's motion intention. However, a robotic anticipation can only approximate the human intended motion. This approximation based on human behavior prediction may disagree with the real human intentions requiring a corrective force from the human side. Due to the impossibility to observe the human's real intentions in advance, we consequently model this input as process noise in the system dynamics, being normally distributed, i.e., $\boldsymbol{u_h} = \epsilon = \mathcal{N}(\boldsymbol{u_0}, \boldsymbol{\Sigma_{u_h}})$. The process noise ϵ can be also interpreted as the *level of disagreement* with the human partner.

As the system is implemented in discrete time, we discretize the system from (1) with a sampling time interval Δt yielding a discretized plant dynamics in the form $\boldsymbol{\xi}_{k+1} = A\boldsymbol{\xi}_k + B\boldsymbol{u_k}$ given by

$$\begin{pmatrix} \boldsymbol{x}_{k+1} \\ \boldsymbol{v}_{k+1} \end{pmatrix} = A \begin{pmatrix} \boldsymbol{x}_k \\ \boldsymbol{v}_k \end{pmatrix} + B(\boldsymbol{u_r}_k + \epsilon_k) \ , \tag{2}$$

where $\boldsymbol{x}_k$, $\boldsymbol{v}_k$ and $\boldsymbol{u_r}_k$ are the discrete time position, velocity and robot control input at time k and

$$A = \begin{pmatrix} 1 & \Delta t \\ 0 & 1 - M_r^{-1} D_r \Delta t \end{pmatrix} \quad B = \begin{pmatrix} 0 & 0 \\ 0 & M_r^{-1} \Delta t \end{pmatrix} \ .$$

In our implementation the process noise characteristics are continuously reestimated as the first and second order moments of $\boldsymbol{u_h}$ over the past W observed samples.

Considering this plant dynamics, two assistive control schemes with different human desired state trajectory $\boldsymbol{\xi}_d$ and process noise models ϵ are designed. On one side a model-based assistance relies on the task model's λ predictions and assumes that the deviations coming from the human side are not diverging from λ's predictions, i.e. the human's goal coincides with the model's description. On the other side, a model-free control assumes that the human diverges from any known task models discarding their predictions. The human desired state trajectory is then estimated based only on the human's control input. As shown in [18], [19], a risk-sensitive optimization arises as a suitable choice for the synthesis of the robotic contribution in this problem setting. Standard optimization methods neglect the variablility induced by human unexpected behavior represented by the process noise. However, a risk-sensitive optimization directly considers this variability consequently adapting the robotic gains while tracking the desired state trajectory $\boldsymbol{\xi}_d$.

A. Model-based control scheme

The model-based scheme assumes that the the behavior represented by the task model λ coincides with the human motion intention and therefore follows the predictions given by λ, i.e. $\boldsymbol{\xi_d} = \hat{\boldsymbol{\xi}}_{\boldsymbol{\lambda}}$. As both partners agree in the path to follow, any disturbances from the human side represented by the process noise ϵ are not diverging from the actual goal. Deviations are assumed to be produced by small prediction errors but no clear divergence is considered. Consequently, in this case the process noise is interpreted as unbiased, i.e. $\epsilon = \mathcal{N}(0, \boldsymbol{\Sigma_{u_h}})$.

B. Model-free control scheme

A model-free control scheme assumes different intended goals between the human and the task model. During physical interaction, this can be detected based on the measured interaction force, where a continuous level of human force input indicates a disagreement to the current motion. In order to represent this divergence, a biased process noise is considered, i.e. $\epsilon = \mathcal{N}(\boldsymbol{u_0}, \boldsymbol{\Sigma_{u_h}})$. Due to the disagreement assumption, the task model prediction is consequently discarded and the human desired trajectory is estimated based on the process noise bias. In this case, the dynamics are given by

$$\boldsymbol{\xi}_{k+1} = A\boldsymbol{\xi}_k + B(\boldsymbol{u_r}_k + \boldsymbol{u_0}_k + \epsilon_k) \ . \tag{3}$$

Applying the system dynamics for the observed bias, the model-free prediction of the desired state trajectory $\boldsymbol{\xi_d} = \hat{\boldsymbol{\xi}}_{\boldsymbol{c}}$ is given by

$$\hat{\boldsymbol{\xi}}_{\boldsymbol{c}k+1} = A\boldsymbol{\xi}_k + B\boldsymbol{u_0}_k. \tag{4}$$

Capturing the effect of the observed bias $\boldsymbol{u_0}$ in the desired trajectory, the process noise is again expressed as unbiased. The model-free control considers the bias estimation as the human desired trajectory, i.e. $\boldsymbol{\xi}_d = \hat{\boldsymbol{\xi}}_{\boldsymbol{c}}$.

C. Risk-sensitive solution

Given a desired trajectory based on human behavior prediction $\boldsymbol{\xi_d}$ and the plant dynamics from (2), the solution for this problem from an optimality point of view is designed by penalizing the distance to the desired trajectory. Due to the continuous reestimation of the process noise characteristics, a model-predictive control scheme is adopted as the problem parameters change. As a consequence, the optimal solution is constantly recalculated. A quadratic cost function at sample time k for this problem takes the form

$$J_k = \sum_{i=k}^{k+T} \|(\boldsymbol{\xi_d}_i - \boldsymbol{\xi}_i)\|_Q^2 + \|\boldsymbol{u_r}_i\|_R^2 \ , \tag{5}$$

where T is the time horizon, $\|x\|_Q^2$ stands for the quadratic form $x^{\mathrm{T}}Qx$ and Q and R are weighting factors that allow a trade-off between control cost and tracking error minimization.

The minimization of the expectation $\mathbb{E}[J_k]$ of the cost function for the dynamics (2) leads to a feedback solution that provides optimal tracking. However, the influence of the process noise ϵ is not considered, i.e. the human's unexpected behavior represented by the process noise's covariance does not influence the tracking gains.

In contrast, a risk-sensitive controller directly considers the process noise in the dynamics, adapting the tracking gains depending on a risk-sensitivity parameter θ. In this case the optimal solution is calculated minimizing the exponential cost function given by

$$\gamma(\theta) = -2\theta^{-1} \ln \mathbb{E}[\exp^{-\frac{1}{2}\theta J_k}] \ , \tag{6}$$

where θ defines the optimization's risk-sensitivity. If $\theta = 0$ the controller is risk-neutral and the process noise has no influence on the optimization. For $\theta < 0$ and $\theta > 0$ the controller becomes risk-averse and risk-seeking, respectively.

The solution to this problem leads to a feedback control law in the form

$$\boldsymbol{u_r}_k = -K_i(\boldsymbol{\xi_d}_i - \boldsymbol{\xi}_i) \ . \tag{7}$$

where K_i is the feedback matrix given by a modified form of the Ricatti recursion [20]

$$K_i = -R^{-1}B'(BR^{-1}B' + \theta\boldsymbol{\Sigma}_{\boldsymbol{u_h}k} + \Pi_{i+1}^{-1})^{-1}A \ ,$$

and

$$\Pi_i = Q_i + A'(BR^{-1}B' + \theta\boldsymbol{\Sigma}_{\boldsymbol{u_h}k} + \Pi_{i+1}^{-1})^{-1}A \ ,$$

with $\Pi_T = Q_T$. Note that due to the model-predictive control scheme, the optimization is solved at each time step k for the updated plant dynamics but only the first step $i = k$ of the optimization's horizon is applied.

The risk-sensitive solution considers the process noise level ϵ influence in the feedback matrix K_i and therefore adapts the robot control gains depending on the disagreement level with the human partner. The risk-sensitive parameter θ determines how the process noise is interpreted. For $\theta < 0$ the process noise influence is seen in a pessimistic way as if it were leading the state in the wrong direction, i.e. under unexpected human behavior variability, the gains increase and the robot becomes stiffer. In contrast, for $\theta < 0$ it is seen as positive influence, i.e. the human variability reduces the gains and the robot becomes less stiff and more compliant adopting a more passive role. See [19] for a detailed explanation of the risk-sensitive solution for assistive robotic assistants.

V. Dynamic Strategy Selection

As already mentioned in the previous section, the principle that governs the control design in this paper is the minimization of the human force contribution during the interaction, which is related to the motion prediction accuracy. A higher prediction accuracy results in a diminished required and applied human force contribution, $\boldsymbol{u_h}$, because it allows the robot to contribute a larger share $\boldsymbol{u_r}$ of the required total force input $\boldsymbol{u}$ to achieve the desired state trajectory $\boldsymbol{\xi_d}$. This motivates us to develop a strategy selector that aims at optimizing the prediction accuracy. By evaluating the models in their short-term retrospective behavior over the window length H, we obtain an estimate for the instantaneous future prediction error. The measure α_i used here to evaluate the prediction accuracy for the control scheme $i \in \{\lambda, c\}$ is defined in the mean squared error sense, i.e.

$$\alpha_{ik} = \frac{1}{H} \sum_{j=k-H+1}^{k} \|\boldsymbol{\xi}_j - \hat{\boldsymbol{\xi}}_{ij}\|^2, \tag{8}$$

where both the model-based and the model-free control strategy simultaneously provide predictions $\hat{\boldsymbol{\xi}}_{\lambda/c}$ of the human desired trajectory. Assuming the prediction error to be stationary within the interval H, α_{ik} defined in (8) serves as a good estimate for the mean squared error of the future prediction based on past observations until time step k, i.e.

$$\mathbb{E}\left[\|\boldsymbol{\xi}_{k+1} - \hat{\boldsymbol{\xi}}_{ik+1}\|^2 | k\right] \approx \alpha_{ik}, \quad i \in \{\lambda, c\}, \tag{9}$$

where $\mathbb{E}\left[x|k\right]$ is the conditional expectation of x conditioned on known data until k. Due to the fact that higher prediction accuracy reduces the human force $\mathbb{E}[\boldsymbol{u_h}]$ and having the estimates for the current prediction accuracy given by (9), we select the applied control scheme $\boldsymbol{u_{r}}_i$ used in the next time step $k+1$ according to the measure α_{ik} by

$$i = \underset{j \in \{\lambda, c\}}{\arg\min}\, \alpha_{j_k}.$$

When choosing a value for the window length H, it can be seen that a trade-off needs to be found between the sensitivity to noise and the ability for fast adaptation to changes of the human behavior. A small value for the window length leads to a greater sensitivity with respect to noise, whereas a large value of H may violate the stationarity assumption needed to assert (9).

Finally, it should be noted that the proposed selection strategy can also be applied to the more general case for N control schemes with $1 \leq i \leq N$, when several model-based schemes are available.

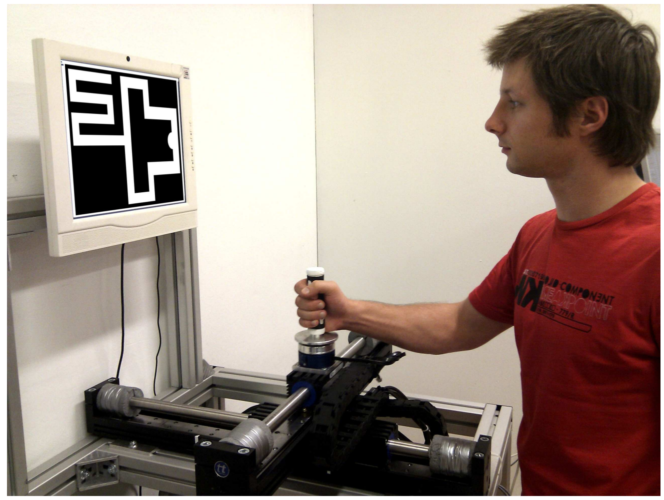

Fig. 2. Cooperative transport of a virtual object through a maze in 2D

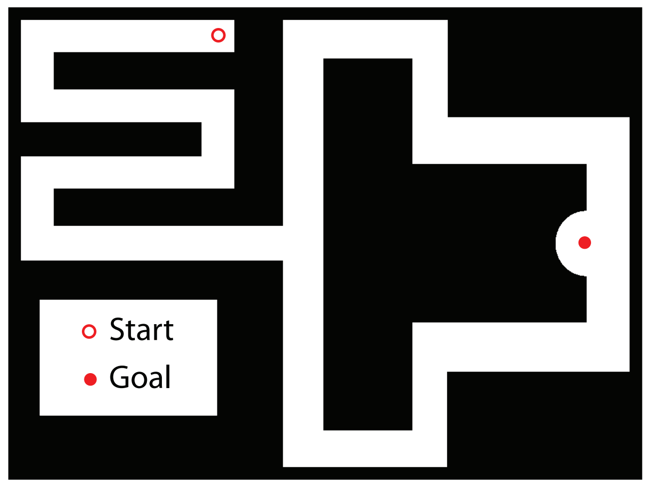

Fig. 3. Example task: Moving a point mass object from start to goal position through a maze

VI. Experimental Evaluation

The proposed control and strategy selection schemes are evaluated in a human-robot cooperative setup in virtual reality. A user study evaluates different assistive control strategies for a simple task consisting of jointly carrying a virtual object from an initial position until a final goal through different possible paths in a 2D maze.

A. Experimental Setup

The virtual-reality interface consists of a two degrees-of-freedom (anteroposterior and mediolateral plane of the user standing in front) linear-actuated device (*ThrustTube*) with a free-spinning handle (superoinferior direction of the user) at the grasp point. The control algorithm is implemented in *Matlab's Simulink Coder* and executed on *Linux Preempt/RT* at a sampling rate of 1 kHz. Attached to the handle is a force/torque sensor (*JR3*), which measures the human force input. The virtual scene is visually represented on a display placed on top of the interface, see Fig. 2. The displayed task

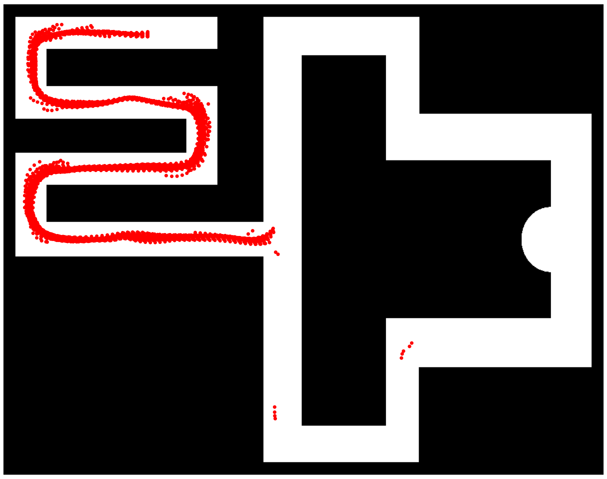

Fig. 4. Spatial distribution of the strategy selection scheme for all participants for the partially known model condition (v): red dots indicate where the model-based strategy was selected.

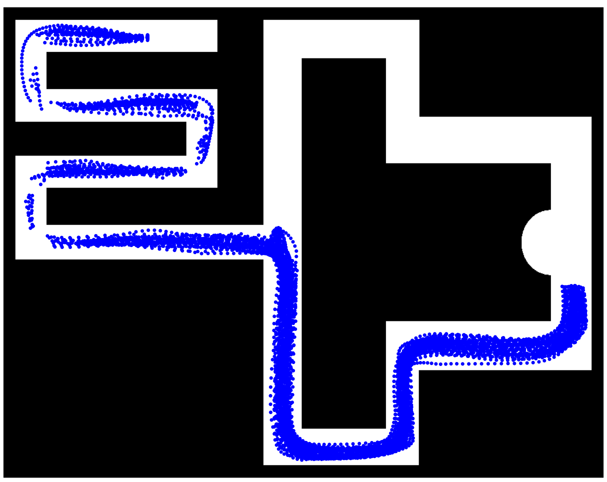

Fig. 5. Spatial distribution of the strategy selection scheme for all participants for the partially known model condition (v): blue dots indicate where the model-free strategy was selected.

to transport a virtual object is visually represented by a filled red circle and the target position in the upper left corner of the maze (blue dot). Collisions with the virtual walls should be avoided. The process noise ϵ_k from (2) is calculated as the first and second order moments of $\boldsymbol{u_h}$ considering a window over the last W observed samples. Table I exhibits the constants used to parameterize the experiment.

B. Quantitative Measures

We evaluate the following criteria in order to rate the performance of the proposed approaches:

- Mean completion time T_{mean} is a task-related performance measure and serves as an indicator of the increase of efficiency to accomplish a task through interaction.
- Mean absolute human force input $\frac{1}{t}\int_0^t \|\boldsymbol{u_h}\|\, d\tau$.
- Mean energy contributed by the human as measure of effort $E = \int_0^t \boldsymbol{u_h}^T \boldsymbol{v}\, d\tau$ is an indicator for the capability of the robotic assistant to take over the overall work load to complete the task.
- Number of collisions with the virtual environment serves as a measure for safety and controllability during task execution.

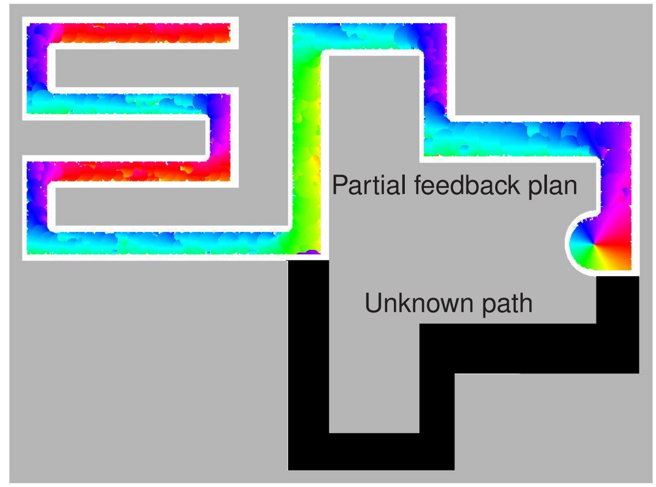

Fig. 6. Feedback motion plan computed with SNG method. The hue indicates the direction towards the goal.

Constant	Equation	Value
Simulated object mass m	(1)	$100\,\text{kg} \cdot I_2$
Simulated viscous friction ν	(1)	$400\,\frac{\text{Ns}}{\text{m}} \cdot I_2$
Process noise window size W	(2)	$0.7\,\text{s}$
Optimization's time horizon T	(5)	$0.1\,\text{s}$
Tracking error weighting Q	(5)	$10^8 I_4$
Control cost weighting R	(5)	I_4
Filter window length H	(8)	$25\,\text{ms}$

TABLE I

CONTROL PARAMETERS USED IN 2-DOF EXPERIMENT

C. Experimental Design

We conducted a small pilot study in the presented VR scenario to evaluate the performance of our proposed approach. Twelve non-paid participants (age mean: 27.5, std: 2.7) were instructed to move a virtual object through the simple maze used above from a starting configuration to a final configuration through the scene without colliding with the virtual obstacles visually and haptically displayed.

A total of 6 different conditions were evaluated depending on the controllers used and the paths chosen to solve the maze

(i) No active assistance, i.e. $\boldsymbol{u_r} = 0$ following always the same path.

(ii) Model-free control scheme with risk-seeking optimization, i.e. $\theta = 10^{-5}$, following always the same path.

(iii) Model-based control scheme with risk-seeking optimization, i.e. $\theta = 10^{-5}$, following always the same path.

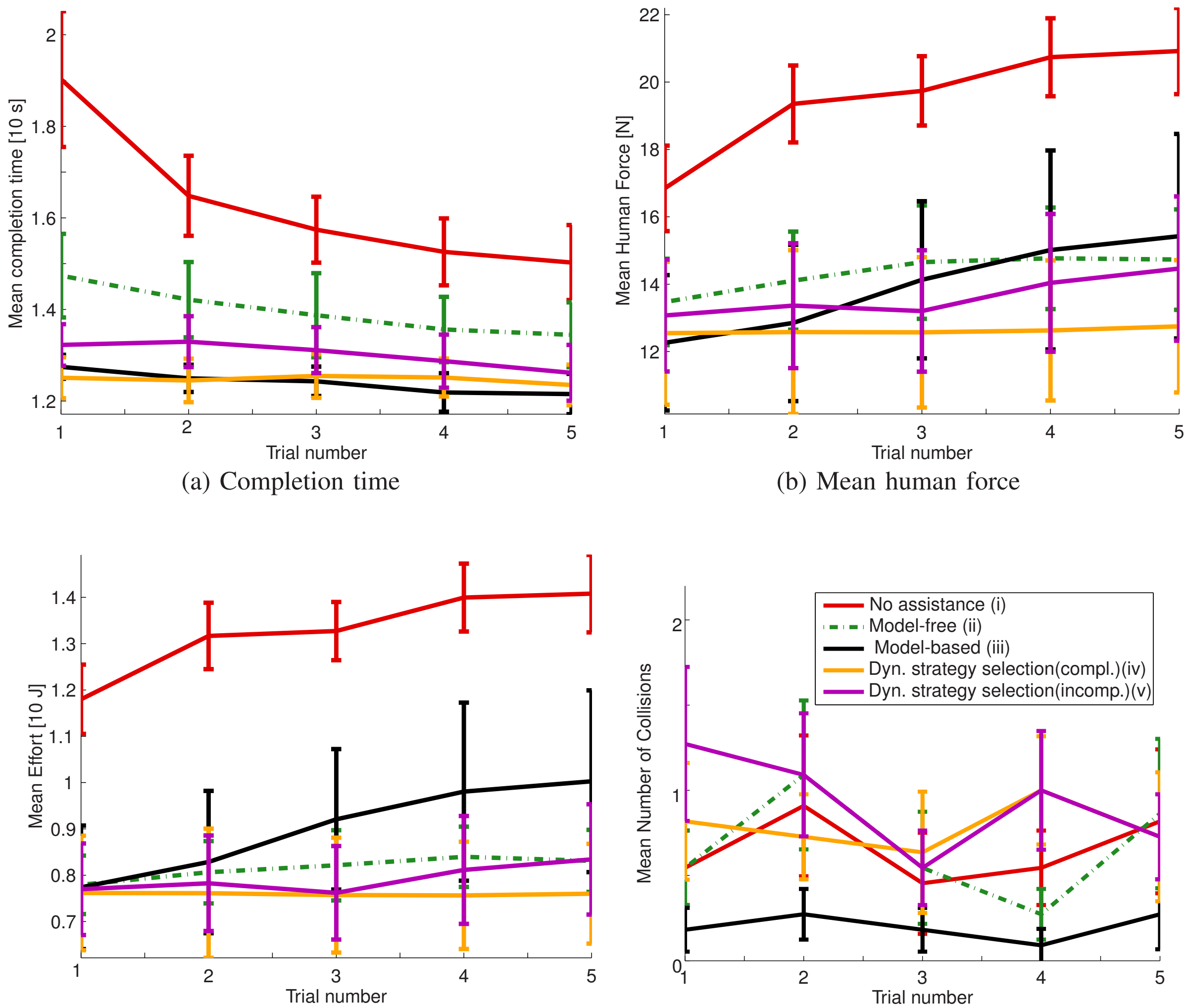

(a) Completion time
(b) Mean human force
(c) Mean absolute power
(d) Mean number of collisions

Fig. 7. Mean and standard deviation evolution of quantitative parameters over trials

(iv) Dynamic strategy selection scheme between controllers (ii) and (iii), following always the same path.

(v) Dynamic strategy selection scheme between controllers (ii) and (iii), following the opposite path with incomplete task model λ.

Each participant repeated each condition 5 times. The underlying task model λ is given by a feedback motion plan towards the goal.

A feedback motion planning algorithm generates a feedback function $\mathcal{K}(\boldsymbol{x})$ for all accessible positions $\boldsymbol{x}$. The sampling-based neighborhood graph (SNG) [21] is a very comprehensible method, efficiently covering the accessible region with the feedback function that indicates the direction towards the goal. Therefore, the entire configuration space is randomly clustered into overlapping circles (or hyperballs in higher dimensions), and Dijkstras algorithm is applied to plan on the connected graph from the circle containing the initial configuration to the circle containing the final configuration. Finding the shortest path within circles is straightforward. The feedback motion plan for our experiment is depicted in Fig. 6. The hue of the colors encodes the direction to the goal. Note, that the lower path is excluded in the feedback plan to render an incomplete task model λ.

D. Experimental Results

The quantitative results of the experiment are depicted in Fig. 7 for all considered conditions. The condition of no assistance (i) has longer completion times and significantly higher mean force and mean absolute power while the mean number of collisions remains on average. While the model-based condition (iii) and the complete strategy selection condition (iv) have similar mean completion times, the mean force and the mean absolute power are higher for condition (iv) as the trial numbers increase, but the mean number of collisions is lower. The model-based condition (iii) has a fixed model and can not adapt its behavior between trials while the complete strategy selection condition (iv) switches from the model-based to the model-free scheme in order to accommodate for higher velocities. Although the path to follow is only partially known, it is remarkable that the incomplete strategy selection condition (v) performs always close to the complete strategy selection condition (iv) for all quantitative measures. At the same time and w.r.t. the model-free scheme (iii), the mean completion time is shorter and the the effort needed lower.

The spatial distribution of the dynamic strategy selection results for the incomplete model case (v) is presented in Fig. 5 and Fig. 4. Figure 5 shows that the model-free control scheme is primarily selected in the unknown area of the map, where the model-based approach has no prior knowledge, and during motion along straight lines, where the model-based approach does not adapt its velocity profile to different execution speeds. The model-based strategy is primarily selected during corner turns, where predictions purely based on the human control input are not successful, see Fig. 4. It is also remarkable that any potentially undesired switching effect (jerk) in the system dynamics was not noticeable for the participants due to the rendered compliance in the linear-actuated device.

The results indicate that our proposed strategy selection scheme combines the advantages of model-based control in case of a suitable task model and the advantages of our proposed model-free control scheme when the task model is far from human motion intention. Model-based control leads to higher execution speed as the trajectory prediction and assistance is accurate not only along straight lines but also during turns. While achieving a similar level of velocity, the proposed dynamic strategy selection scheme requires a significantly lower effort induced by the human partner, an indicator for the efficiency of the strategy.

VII. Conclusions

In this paper we propose a novel control approach for physical robotic assistance to humans applicable in partially known tasks and environmental conditions. A strategy selection scheme dynamically chooses the most suitable control method upon an model-based and model-free assistance. When applied with incomplete or incorrect task knowledge, the dynamic strategy selection scheme automatically selects a model-free scheme to maintain a comfortable level of support to the human. As a result, the advantages of both alternative methods are combined providing better assistance by successfully reducing human effort, as shown by our evaluation in a user study.

The implementation of the proposed approach in a 6D scenario together with the exploitation of the presented dynamic strategy selection scheme with multiple control strategies as well as a larger experiment including more participants and more complex tasks are the matter of our future work.

Acknowledgments

This research is partly supported by the DFG excellence initiative research cluster "Cognition for Technical Systems CoTeSys".

References

[1] N. Sebanz and G. Knoblich, "Prediction in Joint Action: What, When, and Where," *Topics in Cognitive Science*, no. 2, pp. 353–367, 2009.

[2] N. Jarrassé, J. Paik, V. Pasqui, and G. Morel, "How can human motion prediction increase transparency?" in *Proc. IEEE ICRA*, 2008, pp. 2134–2139.

[3] T. Flash and N. Hogan, "The Coordination of Arm Movements: An Experimentally Confirmed Mathematical Model," *J. Neurosci.*, vol. 5, pp. 1688–1703, 1985.

[4] B. Corteville, E. Aertbelien, H. Bruyninckx, J. D. Schutter, and H. V. Brussel, "Human-inspired Robot Assistant for Fast Point-to-point Movements," in *Proc. IEEE ICRA*, 2007, pp. 3639–3644.

[5] S. Miossec and A. Kheddar, "Human motion in cooperative tasks: Moving object case study," in *Proc. IEEE ROBIO*, 2008, pp. 1509–1514.

[6] M. Taïx and D. Flavigné, "Motion Planning with interactive devices," in *Proc. IEEE ECMS*, 2011, pp. 1–6.

[7] M. Lawitzky, J. Medina, and S. Hirche, "Rapid prototyping of planning, learning and control in physical human-robot interaction," in *Proc. International Symposium on Experimental Robotics*, 2012, pp. 819–824.

[8] J. Rosell, C. Vázquez, A. Pérez, and P. Iñiguez, "Motion Planning for Haptic Guidance," *J. Intell. Robotic. Syst.*, vol. 53, no. 3, pp. 223–245, 2008.

[9] C. Vázquez, J. Rosell, L. Chirinos, and O. Domínguez, "Haptic Primitives Guidance Based on the Kautham Path Planner," in *Proc. IEEE/RSJ IROS*, 2010, pp. 4686–4691.

[10] V. Fernandez, C. Balaguer, D. Blanco, and M. Salichs, "Active Human-Mobile Manipulator Cooperation Through Intention Recognition," in *Proc. IEEE ICRA*, 2001, pp. 2668–2673.

[11] A. Thobbi, Y. Gu, and W. Sheng, "Using Human Motion Estimation for Human-Robot Cooperative Manipulation," in *Proc. IEEE/RSJ IROS*, 2011, pp. 2873–2878.

[12] P. Evrard and A. Kheddar, "Homotopy Switching Model for Dyad Haptic Interaction in Physical Collaborative Tasks," in *Proc. EHS EuroHaptics*, 2009, pp. 45–50.

[13] E. Gribovskaya, A. Kheddar, and A. Billard, "Motion Learning and Adaptive Impedance for Robot Control during Physical Interaction with Humans," in *Proc. IEEE ICRA*, 2011, pp. 4326–4332.

[14] J. Medina, M. Lawitzky, A. Mörtl, D. Lee, and S. Hirche, "An Experience-Driven Robotic Assistant Acquiring Human Knowledge to Improve Haptic Cooperation," in *Proc. IEEE/RSJ IROS*, 2011, pp. 2416–2422.

[15] D. Lee and C. Ott, "Incremental kinesthetic teaching of motion primitives using the motion refinement tube," *Auton. Robot.*, pp. 1–17, 2011.

[16] R. Olfati-Saber, A. Fax, and R. Murray, "Consensus and Cooperation in Networked Multi-Agent Systems," *Proc. IEEE*, vol. 95, pp. 215–233, 2007.

[17] L. Parker, "Distributed Intelligence: Overview of the Field and its Application in Multi-Robot Systems," *Jo. Ph. A.*, vol. 2, pp. 5–14, 2008.

[18] J. Medina, D. Lee, and S. Hirche, "Risk Sensitive Optimal Feedback Control for Haptic Assistance," in *Proc. IEEE ICRA*, 2012.

[19] ——, "Disagreement-Aware Physical Assistance Through Risk-Sensitive Optimal Feedback Control," in *Proc. IEEE/RSJ IROS*, 2012.

[20] A. Shaiju and I. Petersen, "Formulas for discrete time LQR, LQG LEQG and minimax LQG optimal control," in *Proc. IFAC*, 2008.

[21] L. Yang and S. LaValle, "The Sampling-Based Neighborhood Graph: An Approach to Computing and Executing Feedback Motion Strategies," *IEEE Trans. Robot. Automat.*, vol. 20, no. 3, pp. 419–432, 2004.